Journal of ELECTRONIC MATERIALS, Vol. 36, No. 2, 2007
DOI: 10.1007/s11664-006-0029-9

Regular Issue Paper

Investigation of the Phase Equilibria of Sn-Cu-Au Ternary and Ag-Sn-Cu-Au Quaternary Systems and Interfacial Reactions in Sn-Cu/Au Couples

YEE-WEN YEN,[1,5] CHIEN-CHUNG JAO,[2,3] HSIEN-MING HSIAO,[2] CHUNG-YUNG LIN,[1,4] and CHIAPYNG LEE[2]

1.—Institute of Materials Science and Technology, National Taiwan University of Science and Technology, Taipei 10672, Taiwan, Republic of China. 2.—Department of Chemical Engineering, National Taiwan University of Science and Technology, Taipei , Taiwan. 3.—Department of Chemical and Materials Engineering, Ta Hwa Institute of Technology, Hsinchu 307, Taiwan, Republic of China. 4.—Department of Chemical Engineering, Chin Min Institute of Technology, Miaoli 351, Taiwan, Republic of China. 5.—E-mail: ywyen@mail.ntust.edu.tw

The phase equilibria of the Sn-Cu-Au ternary, Ag-Sn-Cu-Au quaternary systems and interfacial reactions between Sn-Cu alloys and Au were experimentally investigated at specific temperatures in this study. The experimental results indicated that there existed three ternary intermetallic compounds (IMCs) and a complete solid solubility between AuSn and Cu_6Sn_5 phases in the Sn-Cu-Au ternary system at 200°C. No quaternary IMC was found in the isoplethal section of the Ag-Sn-Cu-Au quaternary system. Three IMCs, AuSn, $AuSn_2$, and $AuSn_4$, were found in all couples. The same three IMCs and (Au,Cu)Sn/$(Cu,Au)_6Sn_5$ phases were found in all Sn-Cu/Au couples. The thickness of these reaction layers increased with increasing temperature and time. The mechanism of IMC growth can be described by using the parabolic law. In addition, when the reaction time was extended and the Cu content of the alloy was increased, the $AuSn_4$ phase disappeared gradually. The (Au, Cu)Sn and $(Cu,Au)_6Sn_5$ layers played roles as diffusion barriers against Sn in Sn-Cu/Au reaction couple systems.

Key words: Phase equilibria, ternary intermetallic compound (IMC), diffusion barrier, isoplethal section

INTRODUCTION

Due to environmental concerns arising from the toxicity of Pb, the European Union (EU) has promulgated directives, which severely restricted the selling of electronic products containing Pb in the EU after July 1, 2006.[1] Several Sn-rich Pb-free solders, such as Sn-Ag, Sn-Cu, Sn-Zn, Sn-Ag-Cu, and Sn-Ag-Bi, have replaced eutectic Sn-Pb solders in microelectronic packaging technology as connecting materials. Among these Pb-free solders, Ag-Sn-Cu ternary and Sn-Cu binary alloys are practical commodities and widely used. The Au is commonly used in flip-chip technology and tape automated bonding as the under bump metallurgy or substrates in printed circuit boards. Ag-Sn-Cu/Au and Sn-Cu/Au joints are frequently formed during soldering processes in electronic products. There are some studies related to interfacial reactions between solders and Au.[2–12] Nakahara et al. studied the reaction of a Sn/Au system at room temperature and found that there were ζ-solid solution, AuSn, $AuSn_2$, and $AuSn_4$ phases between Sn and Au.[6,7] Hannech et al. researched the reaction of Pb-72at.%Sn with Au at 80–160°C, and three intermetallic compound (IMC) layers, AuSn, $AuSn_2$, and $AuSn_4$ phases, were found.[10] Chen and Yen investigated solid/solid interfacial reactions of Sn-Ag/Au systems at various temperatures. They also observed the same three IMC layers.[4] However, no information about Sn-Cu/Au systems can be found.

Phase diagrams are powerful and useful tools to understand interfacial reactions. The constituent binary phase diagrams, Sn-Cu,[13] Sn-Au,[14] and Au-Cu,[15] have

(Received March 30, 2006; accepted October 25, 2006)

been widely studied and published in the literature. With regard to Sn-Cu-Au ternary systems, some studies have been done at different temperatures.[16–24] Karlsen et al. determined the phase relationship of the Sn-Cu-Au system at 360°C and proposed a continuous solid solution between Cu_6Sn_5 and AuSn phases.[18–20] However, Zakel et al. studied the same ternary system at 190°C and found that a two-phase region existed between Cu_6Sn_5 and AuSn phases.[23] Karlsen observed that three ternary IMCs existed in the isothermal section of the Sn-Cu-Au ternary system at 360°C, but Zakel found that there was only one ternary IMC in it at 190°C. Their results were not consistent. The phase equilibria of ternary systems, Au-Sn-Cu,[18–24] Ag-Sn-Cu,[25–34] Ag-Sn-Au,[35–38] and Ag-Cu-Au,[39] at specific temperatures have been published. Regarding the Ag-Sn-Cu-Au quaternary system, no literature is available.

Due to the differing results on the phase equilibria of the Sn-Cu-Au ternary system from different studies and the information on the Ag-Sn-Cu-Au quaternary system being deficient, the isothermal section of the Sn-Cu-Au ternary system and the isoplethal section of the Ag-Sn-Cu-Au quaternary system at a Sn-rich corner will be established at 200°C in this work. No literature was concerned with the interfacial reactions of Sn-Cu/Au systems. The present study focuses on the solid/solid state interfacial reactions in Sn-Cu/Au systems. The kinetics and mechanism of IMC growth are also investigated. Furthermore, the isothermal section of the Sn-Cu-Au ternary system is used to interpret reaction paths of Sn-Cu/Au reaction couples at 200°C.

EXPERIMENTAL PROCEDURES

Phase Equilibria of the Sn-Cu-Au Ternary and Ag-Sn-Cu-Au Quaternary Systems

The alloys for ternary and quaternary phase equilibria experiments were prepared with Sn, Cu, Au, and Ag shots of above 99.9 wt.% purity, and each alloy specimen was of a total mass of 2.0 g. Proper amounts of pure elements were weighed and encapsulated in a quartz tube in a 0.1 N/m^2 vacuum. The sample tube was first placed in a furnace at 900°C for 48 h to ensure a homogeneous liquid mixing of the constituent elements and then quenched in icy water. The quenched sample tubes with Sn-Cu-Au or Ag-Sn-Cu-Au alloys were then annealed at 200°C for 1,000 h so that the equilibrium states of the alloys could be reached. The quartz tubes were quenched in icy water again.

The alloy ingot was removed from the quartz tube and cut into halves. One half of the alloy specimen was for the metallographic analysis, and the other was for the x-ray diffraction (XRD) analysis. An optical microscope (OM) and scanning electron microscope (SEM) were used for microstructure examination, while an SEM with an energy-dispersive spectrometer and electron probe microanalyzer (EPMA) were applied for the compositional analysis. The second half of the alloy specimen was pulverized and analyzed with an x-ray diffractometer to obtain its diffraction pattern. From the JCPDS[40] (Joint Committee of Powder Diffraction Standard) database, phases in the alloy could be identified. Microstructures, compositional data, and diffraction patterns were examined together to identify the phases present in each equilibrated alloy.

Interfacial Reactions in Sn-Cu/Au Couples

Sn-0.3wt.%Cu, Sn-0.5wt.%Cu, Sn-0.7wt.%Cu, and Sn-1.0wt.%Cu alloys were prepared and dealt with using the same procedure listed in the above section except for the annealing process. After quenching, the alloys used for reaction couples were cut into circular disks (6.00-mm diameter and 2.00-mm thickness). The solid/solid state reaction couples were prepared. Two Sn-Cu disks and one Au piece of 3.50 mm × 3.50 mm × 100.00 μm were sandwiched together by two stainless steel screws. The schematic diagram of the reaction couple is similar to a previous work.[4] Boron nitride powders were sprayed on the screws to prevent reactions between the steel and Sn-Cu alloys. The Sn-Cu/Au/Sn-Cu sandwiches fixed with screws were encapsulated in evacuated quartz tubes and placed in a furnace at 150°C, 180°C, or 200°C for periods from 12 h to 400 h. Then, the reaction couple was quenched in icy water.

The reaction couples were mounted in epoxy resin and polished carefully. An OM and SEM were used to observe surface morphologies. The EPMA was used to determine the compositions of IMCs.

RESULTS AND DISCUSSION

Phase Equilibria of the Sn-Cu-Au Ternary System at 200°C

As listed in Table I, 47 Sn-Cu-Au alloys were prepared to survey the phase equilibria of the Sn-Cu-Au ternary system. The alloys were annealed at 200°C for 1000 h. Figure 1a is the backscattered electron image (BEI) micrograph of alloy 1 (Sn-10at.%Cu-10at.%Au). Three different phase regions are observed. The composition of the bright phase is Sn-0.7at.%Cu-19.3at.%Au, which is likely to be the $AuSn_4$ phase [14] with 0.7at.%Cu solubility. The composition of the gray phase is Sn-35.4at.% Cu-15.6at.%Au, which is likely to be Cu_6Sn_5 phase [13] with a great quantity of Au. The third phase region is a dark matrix phase in which the composition is near pure Sn, Sn-0.02at.%Au, and it is likely to be the β-Sn phase. [14] Figure 1b shows the XRD pattern of alloy 1, and the existence of $AuSn_4$, Cu_6Sn_5, and β-Sn phases is confirmed.[40] However, the diffraction peak of the AuSn phase is also observed in Fig. 1b. According to Karlsen's report, a continuous range of homogeneity was found between Cu_6Sn_5 and AuSn at 360°C.[18] It is reasonable to consider that there exists a complete solid solubility between AuSn and Cu_6Sn_5 phases in the Sn-Cu-Au ternary isothermal section at 200°C. In this study, the stoichiometric

Table I. Phase Equilibria of Sn-Cu-Au Ternary Alloys Experimentally Investigated in this Study Annealed at 200°C for 1,000 h—Selected Equilibrium Compositions Listed for Every Phase Region

Alloy No.	Alloy Composition (At.%)				Composition (At.%)		
	Sn	Cu	Au	Phases	Sn	Cu	Au
1*	80	10	10	Sn + $AuSn_4$ + χ	67.1	0.5	32.4
2	70	25	5	$AuSn_2$	79.7	0.8	19.5
				$AuSn_4$	49.2	23.8	27.0
				χ			
3	70	10	20	$AuSn_4$ + χ			
4	70	15	15	Sn + $AuSn_4$ + χ			
5	70	20	10	Sn + χ			
6*	55	10	35	$AuSn_2$ + χ			
7	55	15	30	$AuSn_2$ + χ			
8	55	20	25	$AuSn_2$ + $AuSn_4$ + χ			
9	60	20	20	$AuSn_4$	79.3	0.4	20.3
				χ	51.3	28.6	20.1
10	60	25	15	Sn + $AuSn_4$ + χ			
11	60	35	5	Sn	99.8	0.1	0.1
				χ	46.5	46.3	7.2
12	40	10	50	ζ + χ			
13	40	23	37	C	34.1	33.2	32.7
				χ	50.5	7.9	41.6
14	40	30	30	B + C + χ			
15	40	35	25	B + C + χ			
16	40	43	17	Cu_3Sn + χ			
17	40	55	5	Cu_3Sn	25.1	73.3	1.6
				χ	46.8	47.3	5.9
18	30	18	52	ζ + (Au,Cu) + χ			
19	30	23	47	A	18.7	37.5	43.8
				(Au,Cu)	4.1	47.2	48.7
				χ	49.4	3.7	46.9
20	30	30	40	B	20.1	44.2	35.7
				C	33.2	33.1	33.7
				χ	47.8	6.1	46.1
21*	33	40	27	B + C + χ			
22	30	50	20	B	22.5	57.4	20.1
				Cu_3Sn	24.2	68.1	7.7
				χ	47.5	26.1	26.4
23	25	32	43	A	20.9	34.9	44.2
				B	19.5	42.1	38.4
				χ	48.5	4.8	46.7
24	23	37	40	A + B + χ			
25	23	42	35	B	19.8	45.5	34.7
				C	31.5	33.8	34.7
26	20	10	70	ζ	12.5	12.1	75.4
				χ	48.7	1.5	49.8
27	20	20	60	ζ + χ			
28*	20	25	55	(Au,Cu) + ζ + χ			
29	20	30	50	(Au,Cu)	6.5	43.3	50.2
				χ	48.5	5.1	46.4
30	15	44	41	(Au,Cu) + A + B			
31	19	50	31	(Au,Cu)	6.5	58.7	34.8
				B	19.3	49.5	31.2
32	20	71	9	Cu_3Sn			
33	20	77.5	2.5	(Au,Cu) + Cu_3Sn			
34	8	17	75	(Au,Cu)			
35	10	45	45	(Au,Cu) + A			
36	13	48	39	(Au,Cu) + B			
37	11	60	29	(Au,Cu)	5.6	67.5	26.9
				B	19.3	51.6	29.1
38	13	67.5	19.5	(Au,Cu) + B			
39	15	70	15	(Au,Cu) + B + Cu_3Sn			
40	11	79.5	9.5	(Au,Cu)	4.8	86.8	8.4

Table I. Continued

Alloy No.	Alloy Composition (At.%) Sn	Cu	Au	Phases	Composition (At.%) Sn	Cu	Au
			Cu_3Sn	19.1	71.1	9.8	
41	50.5	41.5	8	Sn + χ			
42	50	32.5	17.5	χ			
43	49	25	26	χ			
44	49	21	30	χ			
45	49	18	33	$AuSn_2$ + χ			
46	48	16	36	C + χ			
47	47	7	46	C + χ			

A—$Au_{46}Cu_{33}Sn_{20}$-$Au_{43}Cu_{37}Sn_{20}$, B—$Au_{35}Cu_{45}Sn_{20}$-$Au_{20}Cu_{60}Sn_{20}$, and C—$Au_{34}Cu_{33}Sn_{33}$-$Au_{32}Cu_{35}Sn_{33}$χ—$Au_{5x}Cu_{6(1-x)}Sn_5$, x: 0–1*The equilibrium compositions are mentioned in the text

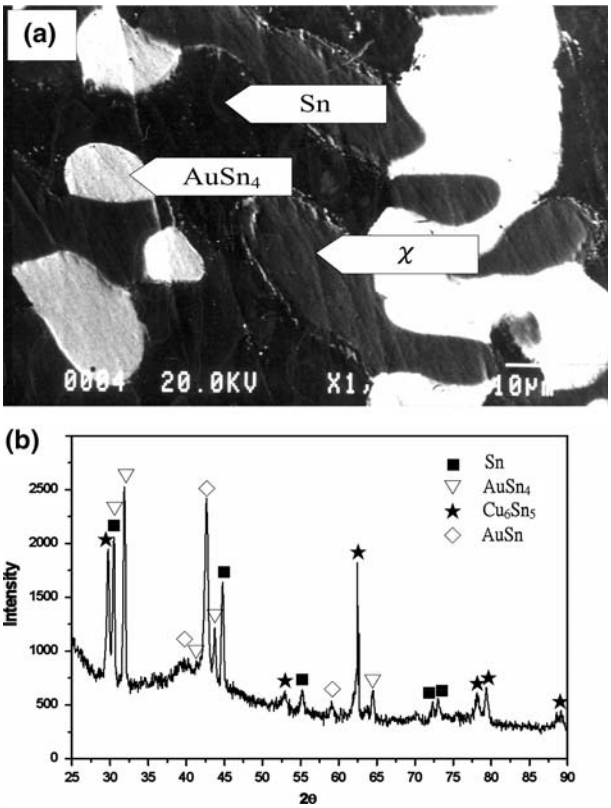

Fig. 1. (a) BEI micrograph and (b) XRD pattern of alloy 1 (Sn-10at.%Cu-10at.%Au) annealed at 200°C for 1,000 h.

formula of this continuous solid solution is expressed as $Au_{5x}Cu_{6(1-x)}Sn_5$, x: 0–1, which is labeled as χ phase. The EPMA and XRD results indicate that the equilibrium phases of alloy 1 at 200°C are $AuSn_4$, χ, and β-Sn. Similar results are found for alloys 4 and 10, and both are in $AuSn_4$, χ, and β-Sn tie-triangle regions.

Figure 2a is the BEI micrograph of alloy 6 (Sn-10at.%Cu-35at.%Au). Two different brightness regions are observed. The compositions of the dark and the gray phases determined by using EPMA are, respectively, Sn-0.5at.%Cu-33.4at.%Au and Sn-12.9at.%Cu-36.4at.%Au, and they are likely to be the $AuSn_2$ and AuSn phases.[14] The XRD pattern of alloy 6 is shown in Fig. 2b. The diffraction peaks of $AuSn_2$ and AuSn phases are observed.[40] However, the diffraction peak of the Cu_6Sn_5 phase is also found in Fig. 2b. Following reasoning similar to that mentioned above, a complete solid solution exists between Cu_6Sn_5 and AuSn phases at 200°C. A similar result is found for alloy 7. Alloys 6 and 7 are in the two-phase regions and there are $AuSn_2$ and χ.

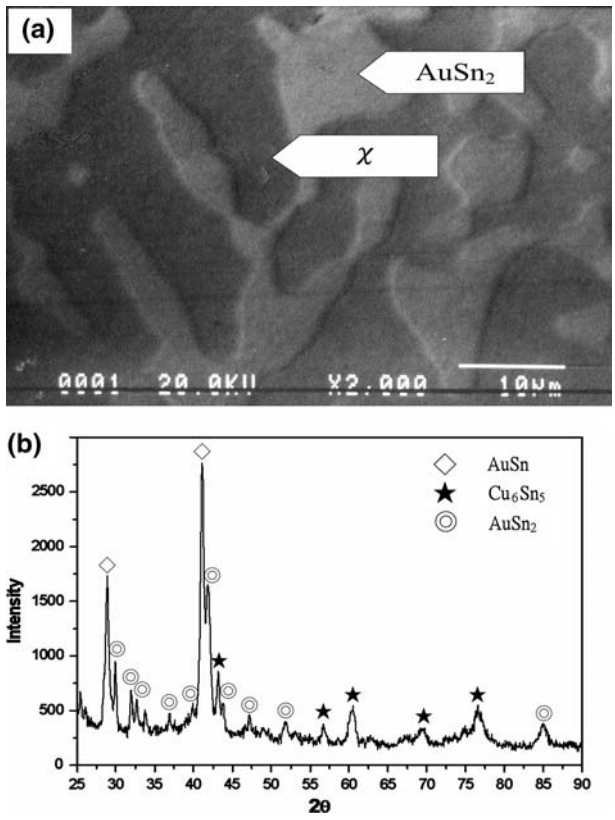

Fig. 2. (a) BEI micrograph and (b) XRD pattern of alloy 6 (Sn-10at.%Cu -35at.%Au) annealed at 200°C for 1,000 h.

Below the χ phase region, 29 alloys (alloys 12 to 40) were prepared to examine the phase relations in this system. The microstructure of alloy 21 (Sn-40at.%Cu-27at.%Au) is shown in Fig. 3a. Three phase regions, dark, gray, and bright, are observed, and their compositions are, respectively, Sn-60at.%Cu-20at.%Au, Sn-25at.%Cu-27at.%Au, and Sn-35at.%Cu-32at.%Au. The dark region is likely to be the ternary IMC-$Au_2Cu_6Sn_2$, which is named B;[18,40] the gray region is likely to be the AuSn phase;[14] and the bright region is another ternary IMC, $Au_{33}Cu_{34}Sn_{33}$, which is named C.[18,40] According to the XRD pattern of alloy 21, as shown in Fig. 3b, the diffraction peaks of B, C, and χ phases are found, and this result is in agreement with the EPMA analyses. As listed in Table I, B, C, and χ are the equilibria for alloys 21, 14, 15, and 20. In alloy 28 , as shown in Fig. 4a, the compositions of three different brightness regions are Sn-43.1at.%Cu-52.6at.%Au (dark), Sn-7.1at.%Cu-48.3at.%Au (gray), and Sn-30.1at.%Cu-58.2at.%Au (light gray). The gray and the light gray regions probably are χ and ζ-solid solution[14] phases, respectively. The dark region is likely the (Au,Cu) phase with a AuCu stoichiometric ratio. However, from the XRD pattern (Fig. 4b), the AuCu peak cannot be found. Similarly, Au_3Cu and $AuCu_3$ are not found in other specimens. There is no inconsistency between the Sn-Cu-Au isothermal sections at 360°C,[19] 190°C,[23] and 200°C, showing that the (Au,Cu) phase is a complete continuous solid solution. In addition, Sato and Toth have shown that about 8at.%Sn has lowered the ordering temperature of the AuCu phase enough to prevent the ordered phases, Au_3Cu, AuCu, and $AuCu_3$, from being formed.[41]

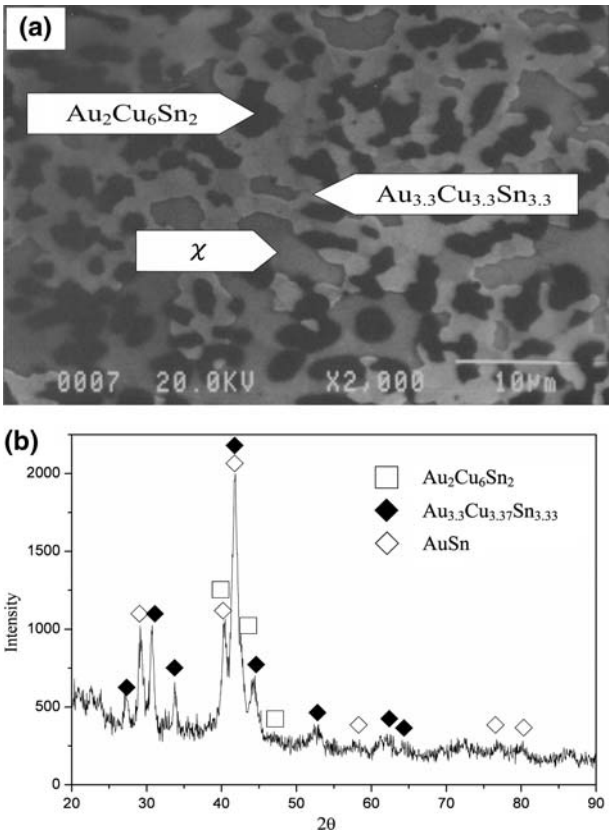

Fig. 3. (a) BEI micrograph and (b) XRD pattern of alloy 21 (Sn-40at.%Cu-27at.%Au) annealed at 200°C for 1,000 h.

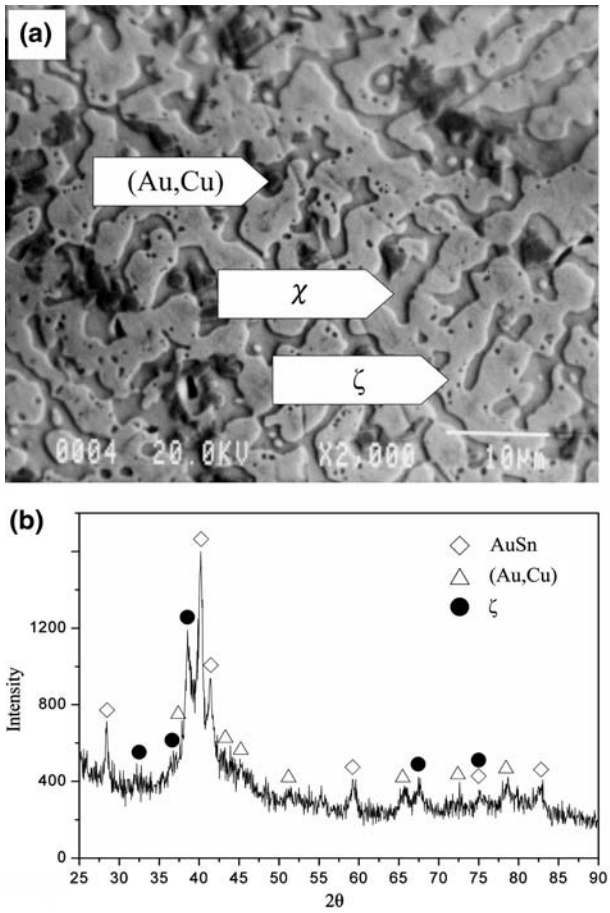

Fig. 4. (a) BEI micrograph and (b) XRD pattern of alloy 28 (Sn-25at.%Cu-55at.%Au) annealed at 200°C for 1,000 h.

For the examination of the continuous solid solution between AuSn and Cu_6Sn_5 phases, seven alloys, alloys 41–47, were prepared in the region, which is around the composition of 50at.%Sn. Figure 5a and b show the BEI micrograph and XRD pattern of alloy 43 (Sn-25at.%Au-26at.%Cu). There is a single-phase morphology in Fig. 5a, but both Cu_6Sn_5 and AuSn phase peaks are shown in Fig. 5b. Due to the study of Karlsen[18] and the same NiAs structure of Cu_6Sn_5 and AuSn phases from JCPDS,[40] it is considered that a single phase was formed in this alloy. Furthermore, based on XRD general principles, the relationship between the composition and lattice parameter is linear in a single-phase region.[38] Results of the XRD analyses for alloys 41–47 are used to calculate the lattice parameters of χ phases by using Bragg's law and the hcp structure relation as the following formulation:[42]

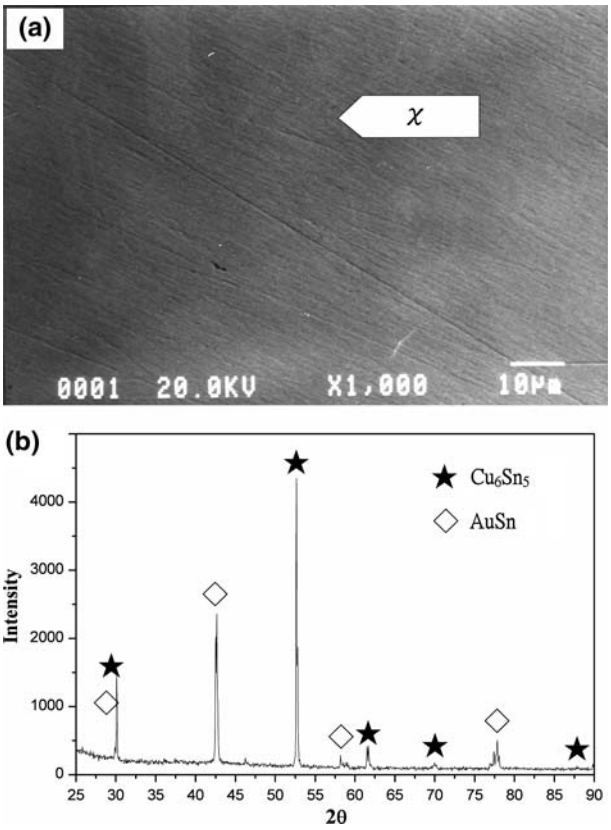

Fig. 5. (a) BEI micrograph and (b) XRD pattern of alloy 43 (Sn-25at.%Au-26at.%Cu) prepared around 50at.%Sn and annealed at 200°C for 1,000 h.

$$\frac{1}{d^2} = \frac{4}{3}\left(\frac{h^2 + hk + k^2}{a^2}\right) + \frac{l^2}{c^2}$$

Figure 6 is a plot of the following lattice parameters: a and c versus the mole ratio of $(n_{Cu}/n_{Cu} + n_{Au})$. The straight in Fig. 6 is found. It indicates that there exists a complete solid solubility between AuSn and Cu_6Sn_5 phases in the isothermal section of the Sn-Cu-Au ternary system at 200°C. This result is similar to Karlsen's[18] at 360°C, but this is not identical with the isothermal section at 190°C proposed by Zakel.[23]

Other alloys were examined, and the results are listed in Table I. Based on experimental determinations of all 47 equilibrated alloys, the isothermal section of the Sn-Cu-Au ternary system at 200°C is proposed and shown in Figure 7. The experimental results indicate that there exist two complete continuous solid solutions in the Sn-Cu-Au ternary isothermal section at 200°C. These two solid solutions are χ and (Cu, Au) phases, respectively. The $AuSn_2$ and the $AuSn_4$ phases have a limited solubility of Cu. However, the ζ phase has a great solubility of Cu, which reaches a level of 28at.%Cu. The Cu_3Sn phase has the solubility of 10at.%Au. Three ternary IMCs, A, B, and C, having

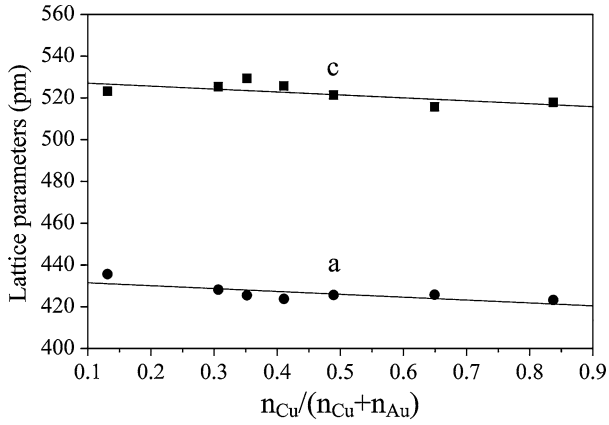

Fig. 6. Lattice parameters a and c versus the mole ratio of $(n_{Cu}/n_{Cu} + n_{Au})$.

the homogeneity ranges $Au_{46}Cu_{33}Sn_{20}$-$Au_{43}Cu_{37}Sn_{20}$, $Au_{35}Cu_{45}Sn_{20}$-$Au_{20}Cu_{60}Sn_{20}$, and $Au_{34}Cu_{33}Sn_{33}$-$Au_{32}Cu_{35}Sn_{33}$, respectively, are found. In addition, there are 10 single-phase regions, 18 two-phase regions, and 10 tie-triangles in the isothermal section at 200°C.

Phase Equilibria of the Ag-Sn-Cu-Au Quaternary System at Sn-Rich Corner at 200°C

Twenty-five Ag-Sn-Cu-Au alloys, alloys 48–72, were prepared to determine the isoplethal section at 95at.%Sn, and their compositions are listed in Table II. All alloys were annealed at 200°C for 1000 h. As shown in Fig. 8a, four different brightness regions are observed in alloy 54 (Sn-2.5at.%Ag-2.25at.%Cu-0.25at.%Au.). Based on the EPMA compositional analysis, the bright granular region having a uniform composition of Sn-0.1at.%Cu-17.0at.%Au is likely to be the $AuSn_4$ phase.[14] The gray granular region having Sn-74.4at.%Ag-0.5at.%Cu-0.1at.%Au is likely to be the Ag_3Sn phase[43] dissolved Cu and Au, which is labeled as $(Ag,Cu,Au)_3Sn$. The composition of the dark region is Sn-0.2at.%Ag-49.4at.%Cu- 3.3at.%Au and is likely to be the Cu_6Sn_5 phase[13] dissolved Au and Ag, which is labeled as $(Cu,Au,Ag)_6Sn_5$. The gray matrix phase is the Sn phase. The XRD results shown in Fig. 8b indicate that there are $AuSn_4$, Ag_3Sn, Cu_6Sn_5, and Sn phases. Similar analyses were examined for other alloys, and the results are shown in Fig. 9.

The isoplethal section of the Ag-Sn-Cu-Au quaternary system at 95at.%Sn at 200°C is also experimentally established. There are 3 two-phase regions, 3 three-phase regions, and 1 four-phase region in this isoplethal section. No quaternary compound is found.

Interfacial Reaction of Sn-Cu/Au Couples

Three different IMC layers, AuSn, $AuSn_2$, and $AuSn_4$, are found on the Sn/Au interface annealed at 200°C for 100 h. The observation is similar to those of Chen and Yen[4] and Hannech et al.[10] However, the different results can be observed as Cu added to Sn reacting with Au. Figure 10a is the BEI

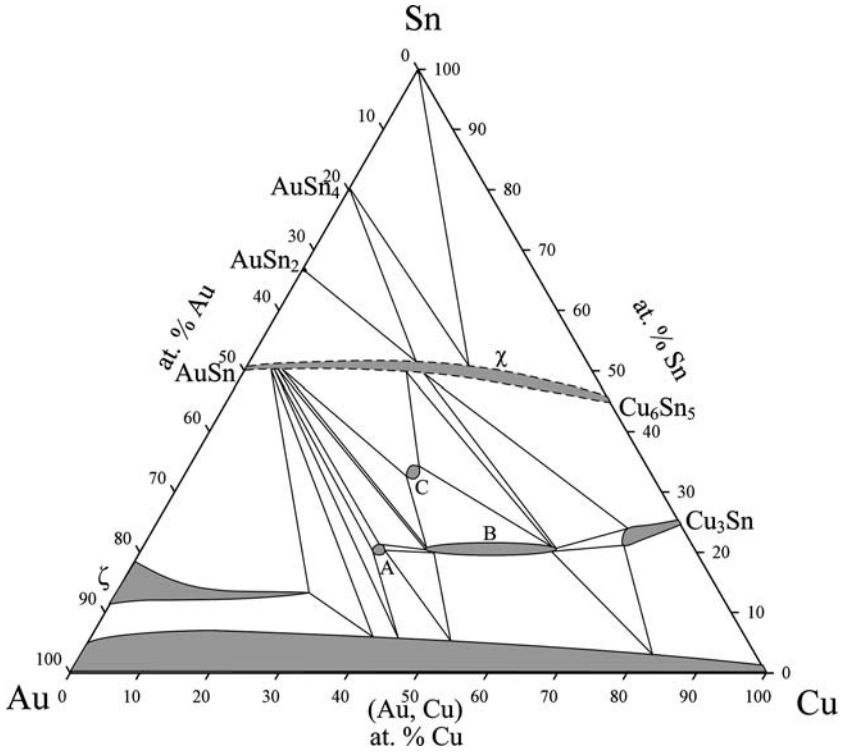

Fig. 7. Isothermal section of the Sn-Cu-Au ternary system at 200°C.

Table II. Phase Equilibria of Ag-Sn-Cu-Au Quaternary Alloys Experimentally Investigated in this Study Annealed at 200°C for 1000 h

Alloy No.	Alloy Composition (At.%)				Phases
	Sn	Au	Cu	Ag	
48	95	0.5	0.5	4	$Sn + Ag_3Sn + AuSn_4$
49	95	0.75	0.75	3.5	$Sn + Ag_3Sn + AuSn_4$
50	95	1.5	0.5	3	$Sn + Ag_3Sn + AuSn_4$
51	95	0.5	1.5	3	$Sn + Ag_3Sn + AuSn_4 + Cu_6Sn_5$
52	95	2.25	0.25	2.5	$Sn + AuSn_4$
53	95	1.25	1.25	2.5	$Sn + Ag_3Sn + AuSn_4 + Cu_6Sn_5$
54	95	0.25	2.25	2.5	$Sn + Ag_3Sn + AuSn_4 + Cu_6Sn_5$
55	95	2	1	2	$Sn + AuSn_4$
56	95	1	2	2	$Sn + Ag_3Sn + AuSn_4 + Cu_6Sn_5$
57	95	3	0.5	1.5	$Sn + AuSn_4$
58	95	1.75	1.75	1.5	$Sn + Ag_3Sn + AuSn_4 + Cu_6Sn_5$
59	95	0.5	3	1.5	$Sn + Ag_3Sn + AuSn_4 + Cu_6Sn_5$
60	95	3	1	1	$Sn + AuSn_4 + Cu_6Sn_5$
61	95	2	2	1	$Sn + Ag_3Sn + AuSn_4 + Cu_6Sn_5$
62	95	1	3	1	$Sn + Ag_3Sn + AuSn_4 + Cu_6Sn_5$
63	95	4	0.5	0.5	$Sn + AuSn_4 + Cu_6Sn_5$
64	95	3	1.5	0.5	$Sn + AuSn_4 + Cu_6Sn_5$
65	95	1.5	3	0.5	$Sn + AuSn_4 + Cu_6Sn_5$
66	95	0.5	4	0.5	$Sn + Ag_3Sn + AuSn_4 + Cu_6Sn_5$
67	95	2.5	0	2.5	$Sn + AuSn_4$
68	95	0	2.5	2.5	$Sn + Ag_3Sn + Cu_6Sn_5$
69	95	2.5	2.5	0	$Sn + AuSn_4 + Cu_6Sn_5$
70	95	1.75	1	2.25	$Sn + AuSn_4$
71	95	3.5	0.5	1	$Sn + AuSn_4$
72	95	0.25	4.5	0.25	$Sn + Ag_3Sn + AuSn_4 + Cu_6Sn_5$

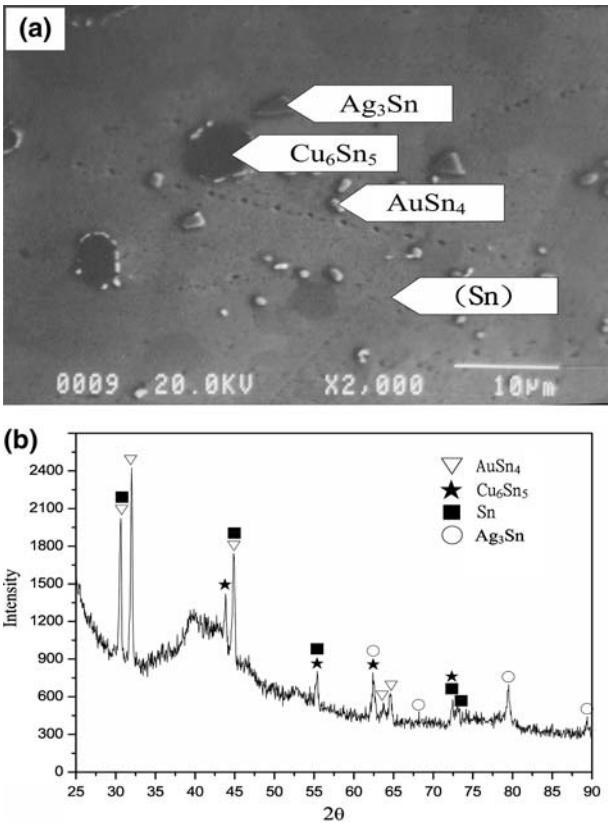

Fig. 8. (a) BEI micrograph and (b) XRD pattern of alloy 54 (Sn-2.5at.%Ag-2.25at.%Cu-0.25at.%Au) annealed at 200°C for 1,000 h.

micrograph of the Sn-0.3wt.%Cu/Au reaction couple annealed at 200°C for 200 h. Except for the above-mentioned three Au-Sn IMC layers, two new layers were formed. The composition of the dark layer is Sn-6.8at.%Au-45.0at.%Cu, which is likely to be the Cu_6Sn_5 phase[13] dissolved Au, and is labeled as $(Cu,Au)_6Sn_5$. The composition of the layer between $(Cu,Au)_6Sn_5$ and $AuSn_4$ is Sn-23.9at.%Au-25.9at.%Cu, which is likely to be the AuSn phase,[14] and is labeled as (Au,Cu)Sn. The similar results of five IMC layers are observed in Sn-0.3wt.%Cu/Au couples annealed at 200°C for various reaction times. However, the category of IMCs will be changed for reaction couples with different Sn-Cu compositions or at various lengths of reaction time. The Sn-1.0wt.%Cu/Au reaction couple was annealed at 200°C for 72 h, as shown in Fig. 10b. There were only four layers on the Sn-Cu/Au interface, and the $AuSn_4$ layer disappeared. Regarding the effect of Cu content for the same length of reaction time, experimental results indicate that the average thickness of IMC is thinner than that of the other reaction couples with lower Cu content in the Sn-Cu alloys. Meanwhile, the thickness of (Au,Cu)Sn and $(Cu,Au)_6Sn_5$ layers is getting thicker. However, in Figs. 10a, b, and 11, there are blurred boundaries and concentration gradients between $(Cu,Au)_6Sn_5$ and (Au,Cu)Sn phases. The morphologies of Fig. 10a and b seemingly disagree with the continuous solid solution between AuSn and Cu_6Sn_5 phases in the isothermal section at 200°C. Maybe two-phase separation between AuSn and Cu_6Sn_5 exists in the χ phase. This phase separation is likely to be narrow and was not found out in this study. In the next work, several alloys will need to be prepared between AuSn and Cu_6Sn_5 to examine the χ phase in detail. In addition, the Sn-Cu/Au and $AuSn/Cu_6Sn_5$ couples will be annealed for more than 300 h to observe the change of boundary between AuSn and Cu_6Sn_5 phases. For different reaction temperatures, such as Fig. 10c that shows

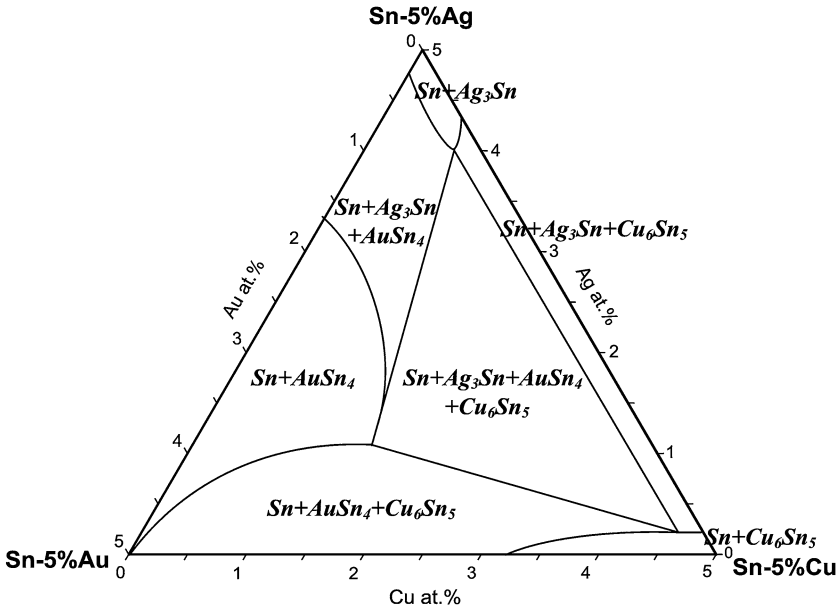

Fig. 9. Isoplethal section of the Sn-Ag-Cu-Au quaternary system with 95at.%Sn at 200°C.

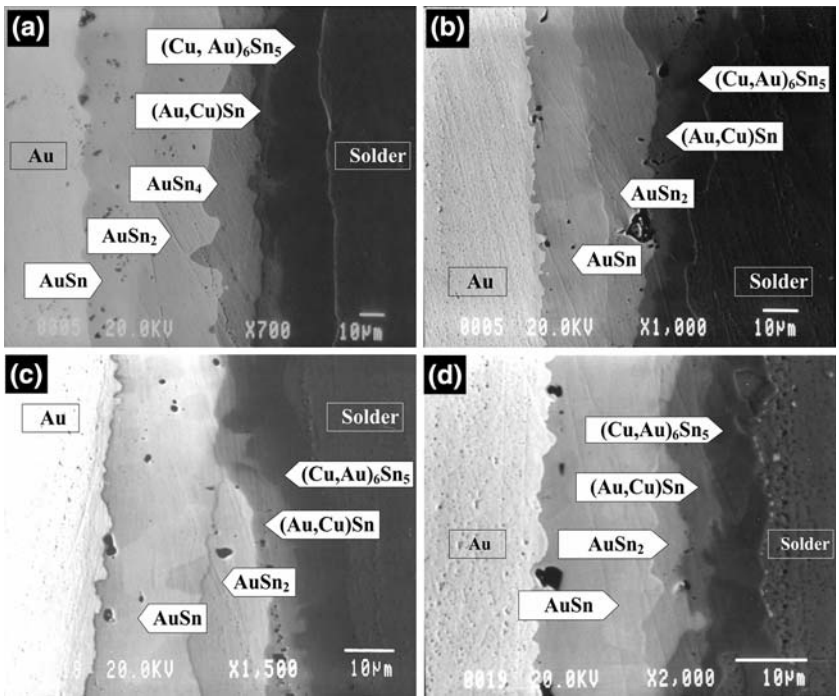

Fig. 10. BEI micrographs of the (a) Sn-0.3wt.%Cu/Au couple reacted at 200°C for 200 h and Sn-1.0wt.%Cu/Au couple reacted at (b) 200°C for 72 h, (c) 180°C for 200 h, and (d) 150°C for 300 h.

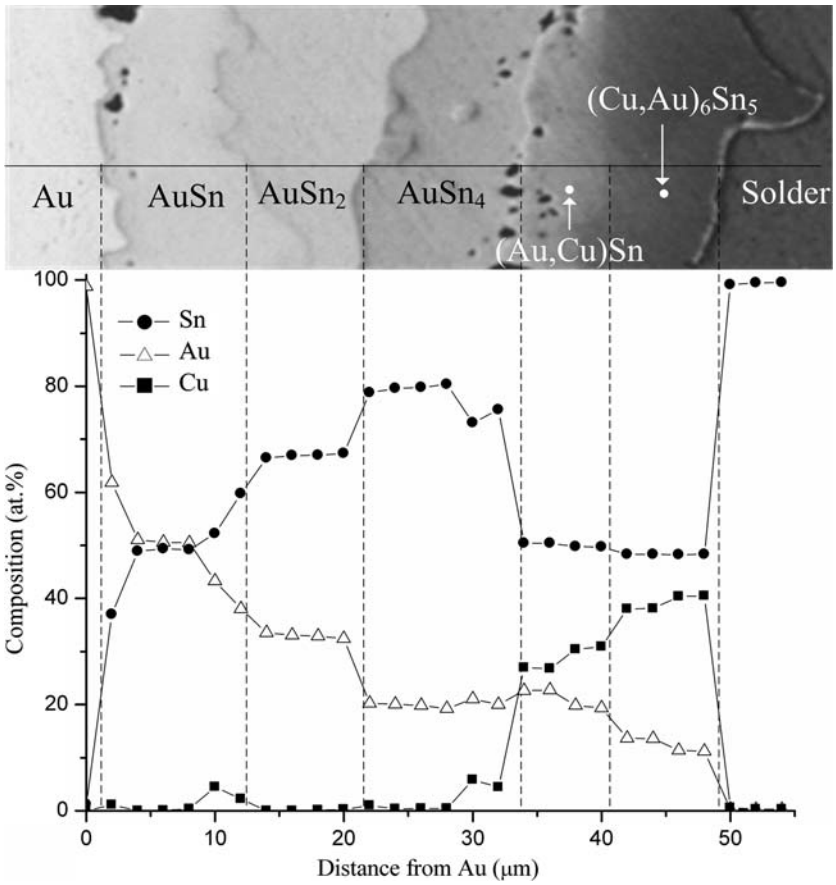

Fig. 11. BEI micrograph and EPMA line-scan compositional profile of the Sn-1.0wt.%Cu/Au couple reacted at 200°C for 24 h.

the morphology of the Sn-1.0wt.%Cu/Au couple annealed at 180°C for 200 h and Fig. 10d that shows the same reaction couple annealed at 150°C for 300 h, there are four different brightness IMC layers, AuSn, $AuSn_2$, (Au,Cu)Sn, and $(Cu,Au)_6Sn_5$, on the Sn-Cu/Au interface in both reaction couples. (Fig. 11)

Table III contains numbers of IMC layers that were formed during interfacial reactions of Sn-Cu/Au couples with different Cu contents and various reaction times at 200°C. When the Cu content and reaction time were increased, the $AuSn_4$ phase gradually disappeared on the interface and turned into (Au,Cu)Sn and $(Cu,Au)_6Sn_5$ phases. Figure 12 is the thickness of total IMC layers of Sn-Cu/Au couples with different Cu contents at 200°C. The total thickness of IMC layers decreased as the Cu content increased, and the slope changed remarkably until the concentration of Cu was more than 0.5 wt.%. Table III and Fig. 12 indicate that Cu added to alloys inhibits the growth of the total IMC layers, although the thickness of $(Cu,Au)_6Sn_5$ increases. The reason seems to be that the (Au,Cu)Sn and $(Cu,Au)_6Sn_5$ layers play roles as diffusion barriers to prevent Sn atoms from diffusing toward Au, which results in the retardation of the Au-Sn IMC growth. The growth of IMC layers can be characterized by the linear relationship between the thickness of IMC and the square root of reaction time, $x = kt^{1/2}$, where k is the growth rate constant. Based on the Arrhenius equation, $k = k_0 \times \exp(-Q/RT)$, the k and the activation energy Q can be determined and shown in Table IV. In Table IV, the lowest activation energy is found in the Sn-0.7wt.%Cu/Au system and the value is 47.51 J/mol. It is likely to be related to the eutectic composition of the Sn-Cu binary system, which is Sn-0.7wt.%Cu.

The possible mechanism of Sn-Cu/Au reaction couples can be explained as follows. In the first step, Sn mainly diffuses into Au to form IMCs of $AuSn_4$, $AuSn_2$, and AuSn. Simultaneously, Cu is concentrated into the Sn-Cu solder on the interface, which results in the formation of the Cu_6Sn_5 phase. The

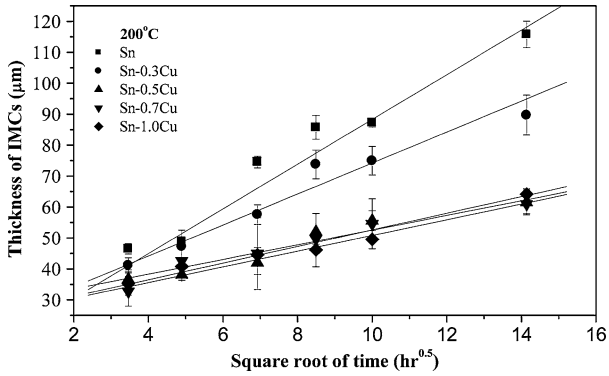

Fig. 12. Thickness of total IMC layers of Sn-Cu/Au couples with different Cu contents at 200°C.

Au also diffuses into the Cu_6Sn_5 phase as $(Cu,Au)_6Sn_5$, which acts as a diffusion barrier against Sn. However, in the early stage of heat treatment, Au content in the $(Cu,Au)_6Sn_5$ phase is not so high (estimated to be less than 20 at.%). Therefore, the $(Cu,Au)_6Sn_5$ phase equilibrates with the $AuSn_4$ phase. Further diffusion of Au into the $(Cu,Au)_6Sn_5$ phase causes the increase of Au content in the $(Cu,Au)_6Sn_5$ phase. When the Au content exceeds the Cu content, the (Au,Cu)Sn phase turns to equilibrate with the $AuSn_2$ phase. That is why the $AuSn_4$ phase disappears. Furthermore, when the Cu content and reaction time increase, for example, the Sn-1.0Ag-2.5Cu/Au couple is annealed at 150°C for 1200 h, one finds that not only the $AuSn_4$ layer but also the $AuSn_2$ layer disappear.[44]

The results in Table III can be tied with the Sn-Cu-Au isothermal section at 200°C to describe the reaction paths of Sn-Cu/Au reaction couple systems. For shorter reaction times and lower Cu contents (<0.5wt.%Cu), the reaction path is Au/AuSn/$AuSn_2$/$AuSn_4$/(Au,Cu)Sn/$(Cu,Au)_6Sn_5$/solder. Otherwise, the reaction path is Au/AuSn/$AuSn_2$/(Au,Cu)Sn/$(Cu,Au)_6Sn_5$/solder for longer reaction times and higher Cu contents. Two kinds of reaction path are shown in Fig. 13. It is clear that the change of Cu

Table III. Numbers of IMC Layers Forming during Interfacial Reactions of Sn-Cu/Au Couples with Different Cu Contents and Various Reaction Times at 200°C

Alloy	Sn	Sn-0.3Cu	Sn-0.5Cu	Sn-0.7Cu	Sn-1.0Cu
Time					
12 h	3	5	5	5	5
24 h	3	5	5	5	5
48 h	3	5	5	5	5*
72 h	3	5	5	5	4
100 h	3	5	5	5*	4
200 h	3	5	5*	4	4

*The $AuSn_4$ phase is not a plane structure; it can only be partially formed at an interface. Three layers: Au/AuSn/$AuSn_2$/$AuSn_4$/Sn. Four layers: Au/AuSn/$AuSn_2$/(Au,Cu)Sn/$(Cu,Au)_6Sn_5$ /solder. Five layers: Au/AuSn/$AuSn_2$/$AuSn_4$/(Au,Cu)Sn/$(Cu,Au)_6Sn_5$/solder.

Table IV. Growth Rate Constants and Activation Energies of Sn-Cu/Au Reaction Couples at Various Reaction Temperatures

	Growth Rate Constant k ($\times 10^{12}$ cm^2/s)			
k	**200°C**	**180°C**	**150°C**	***Q* (J/mole)**
Alloy				
Sn	145.04	45.44	20.30	63.14
Sn-0.3wt.%Cu	69.75	45.40	7.87	74.7
Sn-0.5wt.%Cu	20.00	13.27	2.49	71.28
Sn-0.7wt.%Cu	15.63	10.26	3.81	47.51
Sn-1.0wt.%Cu	17.88	7.84	2.80	60.97

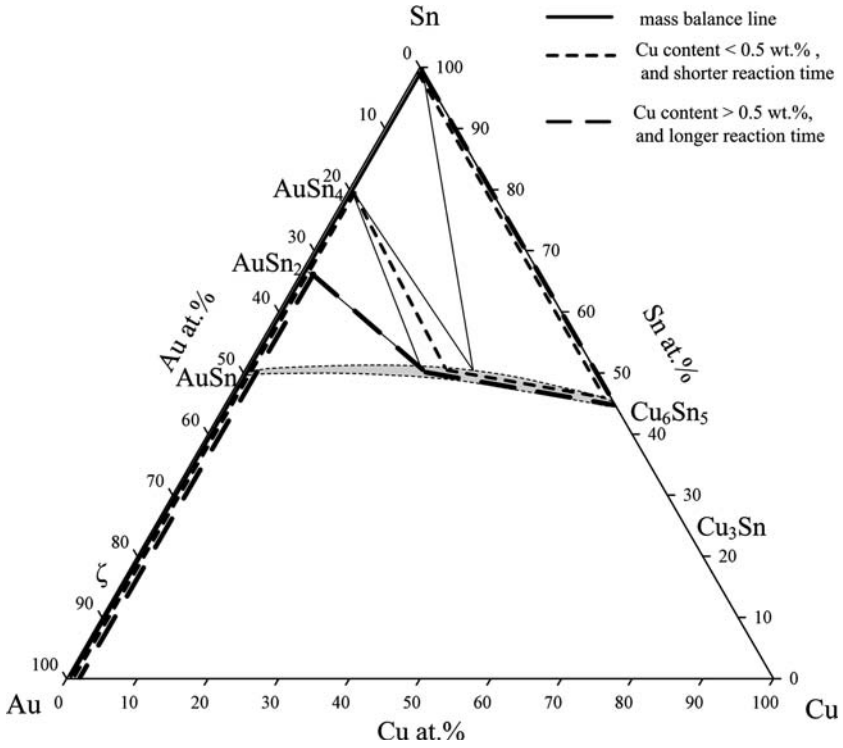

Fig. 13. Reaction paths of Sn-Cu/Au couples reacted at 200°C superimposed with the Sn-Cu-Au 200°C isothermal section.

content affects the formation of IMCs and changes the reaction path in the Sn-Cu/Au reaction couple.

CONCLUSIONS

The isothermal section of the Sn-Cu-Au ternary and the isoplethal section of the Ag-Sn-Cu-Au quaternary system at 200°C are experimentally established. In the Sn-Cu-Au ternary system, there exists two continuous solid solution phases. One is the $Au_{5x}Cu_{6(1-x)}Sn_5$ phase that has a complete solid solubility between AuSn and Cu_6Sn_5 phases and is marked as χ phase, and the other is the (Au,Cu) phase. Three ternary IMCs, A–C are found at 200°C. The Cu atoms could dissolve in the ζ phase in considerable quantities. In the Ag-Sn-Cu-Au quaternary system, no quaternary compound is found.

For all Sn-Cu/Au couples annealed at 200°C less than 48 h, five IMCs, AuSn, $AuSn_2$, $AuSn_4$, (Au,Cu)Sn, and $(Cu,Au)_6Sn_5$, were formed on the interface. The thickness of these reaction layers increased with higher temperature and longer reaction time, and the growth mechanism could be described by using the parabolic law. When the reaction time was extended and the Cu content of an alloy was increased, the $AuSn_4$ layer disappeared gradually. Meanwhile, the formations of AuSn and $AuSn_2$ layers were restrained and (Au,Cu)Sn and $(Cu,Au)_6Sn_5$ became thicker. (Au,Cu)Sn and $(Cu,Au)_6Sn_5$ layers acted as diffusion barriers against Sn in Sn-Cu/Au reaction couple systems. The reaction path of the Sn-Cu/Au couple is Au/AuSn/$AuSn_2$/$AuSn_4$/(Au,Cu)Sn/$(Cu,Au)_6Sn_5$ /solder for short reaction times and lower Cu contents

(<0.5wt.%Cu). Otherwise, for longer reaction times and higher Cu contents, the reaction path is Au/AuSn/$AuSn_2$/(Au,Cu)Sn/$(Cu,Au)_6Sn_5$/solder.

ACKNOWLEDGEMENTS

The authors thank Mr. C.Y. Kao for carrying out the EPMA experiments. The authors acknowledge the financial support of the National Science Council of Taiwan, Republic of China (Grant No. NSC93-2218-E-011-027).

REFERENCES

1. P. Zarrow, Circ. Assembly Aug., 18 (1999).
2. P.G. Kim and K.N. Tu., *Mater. Chem. Phys.* 53, 165 (1998).
3. I. Shohji, S. Fujiwara, S. Kiyono, and K.F. Kobayashi, *Scripta Mater.* 40, 815 (1999).
4. S.W. Chen and Y.W. Yen, *J. Electron. Mater* 30, 1133 (2001).
5. M. Mita, K. Miura, T. Takenaka, M. Kajihara, N. Kurokawa, and K. Sakamoto, *Mater. Sci. Eng. B* 126, 37 (2006).
6. S. Nakahara and R.J. McCoy, *Thin Solid Films* 72, 457 (1980).
7. S. Nakahara, R.J. McCoy, L. Buene, and J.M. Vandenberg, *Thin Solid Films* 84, 185 (1981).
8. D. Gregersen, L. Buene, T. Finstad, O. Lonsjo, and T. Olsen, *Thin Solid Films* 78, 95 (1981).
9. S.K. Sharma, M.P. Singh, and G.I. Malhotra, *Phys. Status Solidi A* 128, 407 (1991).
10. E.B. Hannech and C.R. Hall, *Mater. Sci. Technol.* 8, 817 (1992).
11. P.G. Kim and K.N. Tu, *J. Appl. Phys.* 80, 3822 (1996).
12. J.Y. Tsai, C.W. Chang, Y.C. Shieh, Y.C. Hu, and C.R. Kao, *J. Electron. Mater.* 34, 182 (2005).
13. N. Saunders and A.P. Miodownik, *Bull. Alloy Phase Diagrams* 11, 278 (1990).
14. H. Okamoto and T.B. Massalski, *Bull. Alloy Phase Diagrams* 5, 492 (1984).
15. H. Okamoto, D.J. Chakrabarti, D.E. Laughlin, and T.B. Massalski, *Bull. Phase Diagrams* 8, 454 (1987).
16. J.F. Roder, M.R. Notis, and J.I. Goldstein, *Defect Diffus. Forum* 59, 271 (1988).
17. J.F. Roder (Ph.D. thesis, Lehigh University, 1988).
18. O.B. Karlsen, A. Kjekshus, and E. Røst, *Acta Chem. Scand.* 44, 197 (1990).
19. O.B. Karlsen, A. Kjekshus, and E Røst, *Acta Chem. Scand.* 46, 147 (1992).
20. O.B. Karlsen, A. Kjekshus, C. Rømming, and E. Røst, *Acta Chem. Scand.* 44, 1076 (1992).
21. O.B. Karlsen, A. Kjekshus, C. Rømming, and E. Røst, *Acta Chem. Scand.* 46, 442 (1992).
22. B. Peplinski and E. Zakel, *Mater. Sci. Forum* 166–169, 443 (1994).
23. E. Zakel (Ph.D. thesis, Berlin University of Technology, 1994).
24. J. Kim, *J. Electron. Mater.* 13, 191 (1984).
25. K.W. Moon, W.J. Boettinger, U.R. Kattner, F.S. Blancaniello, and C.A. Handwerker, *J. Electron. Mater.* 29, 1122 (2000).
26. E. Gebhardt and G. Petzow, *Z. Metallkd.* 50, 597 (1959).
27. C.M. Miller, I.E. Anderson, and J.K. Smith, *J. Electron. Mater.* 23, 595 (1994).
28. O. Kubascewski, in Ternary Alloys: a Comprehensive Compendium of Evaluated Constitutional Data and Phase Diagrams, ed. G. Petzow and G. Effenberg (New York: VCH Publishers, 1988).
29. B.J. Lee, N.M. Hawng, and H.M. Lee, *Acta Metall. Mater.* 45, 1867 (1997).
30. H.M. Lee, S.W. Yoon, and B.J. Lee, *J. Electron. Mater.* 27, 1161 (1998).
31. I. Ohnuma, M. Miyashita, K. Anzai, X.J. Liu, H. Ohtani, R. Kainuma, and K. Ishida, *J. Electron. Mater.* 29, 1137 (2000).
32. M.E. Loomans and M.E. Fine, *Metall. Mater. Trans. A* 31A, 1152 (2000).
33. J.Y. Park, C.U. Kim, T. Carper, and V. Puligandla, *J. Electron. Mater.* 32, 1297 (2003).
34. Y.W. Yen and S.W. Chen, *J. Mater. Res.* 19, 2298 (2004).
35. D.S. Evans and A. Prince, in *Phase Diagrams of Ternary Gold Alloys*, ed. A. Prince, G. V. Raynor, and D.S. Evans (London: Institute of Metal, 1990).
36. D.S. Evans and A. Prince, *Met. Sci.* 8, 286 (1974).
37. T.B. Massalski and H. Pops, *Acta Metall. Mater.* 18, 961 (1971).
38. M.L. Malhotra and K.R. Lawless, *J. Biomed. Mater. Res.* 9, 197 (1975).
39. D. de Fontaine, *Metall. Trans. A* 12A, 559 (1981).
40. *JCPDS-International Centre for Diffraction Data* (Swarthmore, PA: American Ceramic Society, 2003).
41. H. Sato and R.S. Toth, *Phys. Rev.* 124, 1833 (1961).
42. B.D. Cullity and S.R. Stock(2001) Elements of X-Ray Diffraction, 3rd ed Prentice Hall, Upper Saddle River, NJ, .
43. I. Karakaya and W.T. Thompson, *Bull. Alloy Phase Diagrams* 8, 340 (1987).
44. C.C. Jao and Y.W. Yen, *Int. J. Mater. Res.* in revision (2006).